



ChemComm

**O₂ Reduction via Concerted-Proton Electron Transfer by a
V(III) Aquo on a Polyoxovanadate-alkoxide Cluster**

Journal:	<i>ChemComm</i>
Manuscript ID	CC-COM-03-2024-001331.R2
Article Type:	Communication

SCHOLARONE™
Manuscripts

O₂ Reduction via Proton-Coupled Electron Transfer by a V(III) Aquo on a Polyoxovanadate-alkoxide Cluster

Shannon E. Cooney,^{a†} Eric Schreiber,^{a†} Baela M. Ferrigno,^a and Ellen M. Matson^{*a}

Received 00th January 20xx,
Accepted 00th January 20xx

DOI: 10.1039/x0xx00000x

We report the transfer of H-atoms from a reduced polyoxovanadate alkoxide [nOct₄N][V₆O₆(OH₂)(OMe)₁₂] via concerted proton-electron transfer. Oxygen reduction is compared between bridging and terminal O-H bonds revealing similar mechanisms, providing new insight to design criteria for metal-oxide electrocatalysts that facilitate oxygen reduction by concerted-proton electron transfer.

Hydrogen fuel cells (HFCs) are promising technologies for renewable electrical energy due to their zero carbon emissions. With the paired employment of the hydrogen oxidation and oxygen reduction reactions (HOR and ORR, respectively), electrical energy is created with water as the sole waste product. ORR is considered the bottleneck to the widespread adoption of HFCs due to its sluggish kinetics.^{1, 2} Currently, to meet performance levels necessary for HFC technologies, high loadings of precious metal catalysts (typically Pt) are required, rendering these systems prohibitively expensive.³ Thus, the development of inexpensive, high-performing cathode materials is necessary.

An alternative class of catalysts that has been demonstrated to facilitate ORR are reducible metal oxides (MO_x).⁴⁻⁶ Despite the library of oxides competent for ORR, the scale and heterogeneity of MO_x renders direct mechanistic determination of the net 4H⁺/4e⁻ reaction challenging, hindering further advances in the optimization (*e.g.* efficiency, selectivity) of MO_x derived catalysts.

To study metal oxide-mediated small molecule activation hydrogenation chemistries with atomic precision, our lab and others have turned to a class of molecular analogues called polyoxometalates (POMs).⁷⁻¹¹ These clusters feature similar composition and surface structure to nanoscopic and bulk MO_x, rendering them ideal platforms for the investigation of reactions and mechanisms at MO_x surfaces. With respect to the ORR, it is well established that exposure of reduced POMs to air results in cluster re-oxidation.^{12, 13} However, relatively little is

known about the mechanism(s) of ORR at the surface of these assemblies.¹⁴ A notable example of ORR by a reduced POM comes from Weinstock and coworkers, where a reduced, Keggin-type polyoxotungstate, [AlW₁₂O₄₀]⁶⁻, reduces O₂ via proton-coupled electron transfer (PCET).¹⁵ The multi-site PCET to form H₂O₂ occurs by initial electron transfer from the cluster followed by proton transfer from the acidic surrounding media (ET-PT). Subsequent work from our laboratory demonstrated the use of a 6H⁺/6e⁻ reduced complex, [V₆O₇(OH)₆(TRIS^{NO2})₂]²⁻, (**Figure 1**) for ORR to H₂O in acetonitrile through a series of concerted proton-electron transfer (CPET) steps.¹⁶

Recently, we reported the *in situ* generation of a reduced POV-alkoxide via addition of two H-atom equivalents to [nOct₄N][V₆O₇(OMe)₁₂] (**1-V₆O₇¹⁻**), yielding a cluster hypothesized to feature a terminal V^{III}-OH₂, [nOct₄N][V₆O₆(OH₂)(OMe)₁₂]¹⁻ (**2-V₆O₆(OH₂)¹⁻**; Scheme 1).¹⁷ The BDFE(O-H)_{avg} values of **2-V₆O₆(OH₂)¹⁻** are similar to the reported values for the bridging hydroxides of [V₆O₇(OH)₆(TRIS^{NO2})₂]²⁻ (59.9 and 61.6 kcal mol⁻¹, respectively), rendering the thermodynamics of small molecule hydrogenation comparable

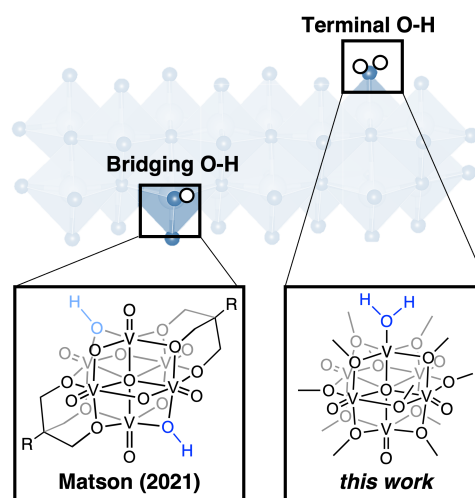
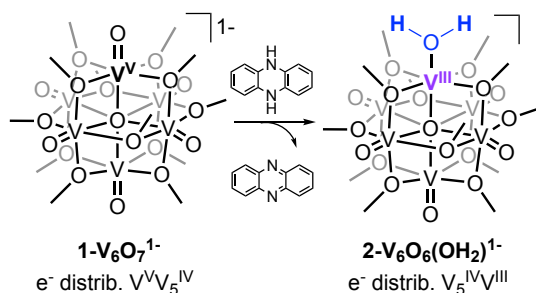


Figure 1. H-atom uptake at POV-alkoxide clusters that model MO_x surfaces. Reducing equivalents can be isolated to bridging and terminal oxide sites at the surface of POV-alkoxides. Blue spheres represent O-atoms while white sphere represent H-atoms.

^a Department of Chemistry, University of Rochester, Rochester NY 14627, USA.

[†] SEC and ES contributed equally to this work.

Electronic Supplementary Information (ESI) available: Synthetic and other experimental procedures, spectroscopic data, kinetic analyses for the oxidation of **2-V₆O₆(OH₂)¹⁻** with TEMPO and O₂. See DOI: 10.1039/x0xx00000x

Scheme 1. Synthesis of $2\text{-V}_6\text{O}_6(\text{OH}_2)^{1-}$.

for the clusters that possess disparate sites (*e.g.* terminal vs. bridging).^{16, 17} We thus became interested in understanding the reactivity of $2\text{-V}_6\text{O}_6(\text{OH}_2)^{1-}$ toward small molecule hydrogenation reactions, as comparison of the reactivity between the two systems would provide an opportunity to examine the effect of the *location* of surface O-H moieties on the mechanism and kinetics of PCET from POV-alkoxides.

Complex $2\text{-V}_6\text{O}_6(\text{OH}_2)^{1-}$ can be isolated by addition of an equivalent of 5, 10-dihydrophenazine to $1\text{-V}_6\text{O}_7^{1-}$ in THF.^{17, 18} The ^1H NMR spectrum of the product features an asymmetric feature at 26.0 ppm and a symmetrical signal at -14.9 ppm; these features are consistent with reduction in cluster symmetry upon formation of a site-differentiated V^{VIII} center (Figure S1).^{19, 20} Analogous reactions performed on the $1e^-$ oxidized cluster, $\text{V}_6\text{O}_7(\text{OMe})_{12}$, have been shown to result in formation of a POV-alkoxide bearing a single $\text{V}^{\text{VIII}}\text{-OH}_2$ moiety, $\text{V}_6\text{O}_6(\text{OH}_2)(\text{OMe})_{12}$.²¹ Attempts to obtain crystals of $2\text{-V}_6\text{O}_6(\text{OH}_2)^{1-}$ were unsuccessful due to the greasy counterion required to maintain solubility of the aquo-ligated cluster. Thus, we rely on the following spectroscopic and reactivity analyses to support the formation of the terminal aquo.

The infrared (IR) spectrum of $2\text{-V}_6\text{O}_6(\text{OH}_2)^{1-}$ reveals features corresponding to the O-CH₃ and V=O stretching modes (1042 and 953 cm^{-1} , respectively; Figure S2). An additional broad, weak band at 3429 cm^{-1} is observed, assigned to the O-H stretch of the bound water molecule. We note that this feature is not present in IR spectrum of the MeCN adduct of the O-atom deficient assembly, $[\text{V}_6\text{O}_6(\text{MeCN})(\text{OMe})_{12}]^{1-}$.¹⁹ Additional evidence of the delivery of two H-atom equivalents to the cluster surface is observed upon inspection of the electronic absorption spectra (EAS) of the POV-alkoxide clusters (Figure S3).¹⁸ The parent cluster, $1\text{-V}_6\text{O}_7^{1-}$, has a prominent feature in the near-IR region ($\lambda_{\text{max}} = 1265 \text{ nm}$, $\epsilon = 937 \text{ M}^{-1}\text{cm}^{-1}$), due to intervalence charge transfer (IVCT) between the V^{IV} and V^{V} in the assembly. This band is quenched upon $2e^-/2\text{H}^+$ reduction, with the only NIR band being a weak d-d transition at 1010 nm ($\epsilon = 138 \text{ M}^{-1}\text{cm}^{-1}$). The absorption spectrum of the reduced assembly possesses a transition at 519 nm ($\epsilon = 1137 \text{ M}^{-1}\text{cm}^{-1}$), with an extinction coefficient that is significantly greater than the corresponding band of $[\text{V}_6\text{O}_6(\text{MeCN})(\text{OMe})_{12}]^{1-}$ ($\lambda_{\text{max}} = 518 \text{ nm}$; $\epsilon = 180 \text{ M}^{-1}\text{cm}^{-1}$). We suggest that intensity of this band is related to the changes in ligand field imparted by the aquo on the d-d transition. Finally, the presence of a terminal aquo

moiety is confirmed from the reaction of $2\text{-V}_6\text{O}_6(\text{OH}_2)^{1-}$ with MeCN, where the water signal is shown to grow over time as MeCN binds to the reduced vanadium centre (Figure S4).

Having successfully generated the aquo-ligated POV-alkoxide, we next turned to H-atom transfer from $2\text{-V}_6\text{O}_6(\text{OH}_2)^{1-}$. TEMPO (2,2,6,6-tetramethyl-1-piperidinyloxy), (TEMPO-H BDFE(O-H) = 65.5 kcal mol^{-1}), serves as an excellent model for H-atom abstraction due to the fact that this substrate is difficult to reduce, and is unlikely to be protonated by the moderately basic $2\text{-V}_6\text{O}_6(\text{OH}_2)^{1-}$.^{18, 22, 23} This leaves the most likely pathway for oxidation of $2\text{-V}_6\text{O}_6(\text{OH}_2)^{1-}$ as CPET. Exposure of two equivalents of TEMPO to $2\text{-V}_6\text{O}_6(\text{OH}_2)^{1-}$ results in quantitative formation of $1\text{-V}_6\text{O}_7^{1-}$, as indicated by ^1H NMR spectroscopy (Figure S5–S6). Kinetic investigations were performed by monitoring the reaction progression *via* EAS, through the method of initial rates (see ESI for more information). The reaction is found to proceed through a rate determining step that is first order in cluster, $2\text{-V}_6\text{O}_6(\text{OH}_2)^{1-}$, and first order in TEMPO with an overall experimentally derived rate constant of $0.15 \pm 0.01 \text{ M}^{-1} \text{ s}^{-1}$ (Figure S7–S10; see ESI for more details).

Next, we conducted variable temperature kinetic experiments to determine the activation parameters of oxidation of $2\text{-V}_6\text{O}_6(\text{OH}_2)^{1-}$ by TEMPO (Figure 2). These experiments have been shown to be valuable for assessing mechanisms of PCET reactions (Figure S11).^{24–27} For the oxidation of $2\text{-V}_6\text{O}_6(\text{OH}_2)^{1-}$, a large and negative value for the entropy of activation ($\Delta S^\ddagger = -41 \pm 8 \text{ cal mol}^{-1} \text{ K}^{-1}$) is consistent with an ordered, bimolecular, H-bonded intermediate invoked in CPET mechanisms.^{18, 27–30} Accordingly, small enthalpy of activation ($\Delta H^\ddagger = 6 \pm 2 \text{ kcal mol}^{-1}$) suggests stabilization by an H-bonded complex in the activated state, in range of ΔH^\ddagger values reported for CPET in metal oxide complexes.^{18, 24–28} These studies demonstrate that $2\text{-V}_6\text{O}_6(\text{OH}_2)^{1-}$ is capable of transferring H-atoms via CPET.

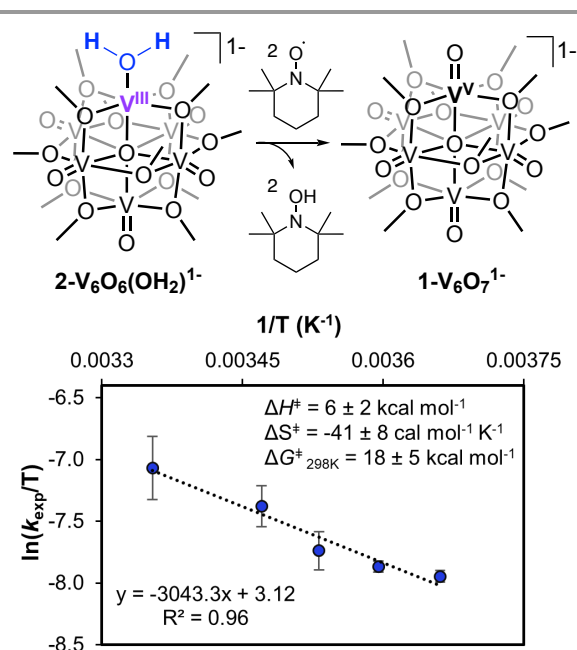


Figure 2. Oxidation by TEMPO (top), Eyring plot for the reaction of 0.30 mM $2\text{-V}_6\text{O}_6(\text{OH}_2)^{1-}$ and 10 mM TEMPO, 0–25 °C.

After establishing the mechanism of H-atom transfer from **2-V₆O₆(OH₂)¹⁻** as CPET, we investigated the reactivity and mechanism of cluster-mediated O₂ reduction. Exposure of **2-V₆O₆(OH₂)¹⁻** to 1 atm of O₂ results in quantitative formation of **1-V₆O₇¹⁻** and 1 equiv of water, as confirmed by ¹H NMR spectroscopy (Figure S12). In our work investigating ORR by [V₆O₇(OH)₆(TRIS^{NO2})₂]²⁻, H₂O₂ was observed prior to the formation of water. Similarly, for **2-V₆O₆(OH₂)¹⁻**, at early time points (~80 s), we observe a signal at 9.37 ppm as the cluster is oxidized, which is consumed by 910 s (Figure S13). To confirm the assignment of this resonance as H₂O₂, we performed trapping experiments using triphenylphosphine (PPh₃).^{31, 32} Importantly, PPh₃ is unreactive toward O₂ and **1-V₆O₇¹⁻** under these conditions, meaning any OPPh₃ formation is solely due to the presence of H₂O₂ produced *in situ* (Figure S14 – S17).²⁰ Upon exposure of cluster to O₂ in the presence of PPh₃, the generation of OPPh₃ is observed, suggesting that ORR by **2-V₆O₆(OH₂)¹⁻** proceeds through an H₂O₂ intermediate.

H₂O₂ formation upon exposure of **2-V₆O₆(OH₂)¹⁻** to O₂ is made possible due to the relative strength of the O-H bonds formed in the product (BDFE(O-H)_{avg} = 69 kcal mol⁻¹ in water) in comparison with those of **2-V₆O₆(OH₂)¹⁻**.²³ This suggests that substrate activation is proceeding through PCET from the V^{III}-OH₂ moiety.²³ This result differs to prior work from our laboratory that has described the mechanism of reoxidation of O-atom deficient POV-alkoxide clusters by O₂ as proceeding through a Mars-van-Krevelen-type mechanism.^{19, 33} Following this route, bifurcation of the O-O bond through interaction of the substrate with an exposed V^{III} site (formed following the dissociation of solvent) results in oxidation of the assembly.

We next turned to kinetic analyses to elucidate the mechanism of ORR by **2-V₆O₆(OH₂)¹⁻**. ORR was monitored by EAS, following the procedure described previously (Figure 3 and Figures S18 – S22; see ESI for details). To determine the order with respect to **2-V₆O₆(OH₂)¹⁻**, we performed reactions under pseudo-first order conditions by adding an excess of O₂ (Figure 3, inset). Results suggest a rate expression for ORR described as: rate = $k_{\text{exp}}[\mathbf{2-V_6O_6(OH_2)^{1-}}][\text{O}_2]$. From the intercept of the line, the experimentally derived second order rate constant, k_{exp} , can be extracted to ($k_{\text{exp}} = 0.061 \pm 0.008 \text{ M}^{-1} \text{ s}^{-1}$). The observed rate for ORR by **2-V₆O₆(OH₂)¹⁻** is significantly accelerated compared to the MeCN bound assembly, V₆O₆(MeCN)(OMe)₁₂⁰, which is oxidized over the course of 8 days (Figure S23).

Next, we considered the possible mechanisms of H-atom transfer from the cluster to O₂. Initial proton transfer to O₂ is thermodynamically disfavoured.³⁵ Instead, transfer of a net H-atom (H⁺/e⁻) to O₂ occurs through either CPET or ET-PT. Such stepwise mechanisms are invoked for catalysts that enable ORR; initial ET is observed by either an outer or inner-sphere mechanism to form O₂⁻, followed by protonation by the surrounding solvent media.³⁵ However, in the case of **2-V₆O₆(OH₂)¹⁻** we observed no evidence of ET. *In situ* analysis of the reaction progression following addition of O₂ to **2-V₆O₆(OH₂)¹⁻** by ¹H NMR spectroscopy shows no formation of the one electron oxidized **2-V₆O₆(OH₂)¹⁻**, V₆O₆(OH₂)(OMe)₁₂⁰ (Figure S13). This is consistent with the fact that **2-V₆O₆(OH₂)¹⁻** lacks sufficient driving force ($E_{\text{ox}} = -0.67 \text{ V}$ vs Fc^{+/0}) to readily perform

ET to O₂ ($E_{\text{Red}} = -1.25 \text{ V}$ vs Fc^{+/0}).^{21, 36} We consequently propose that ORR by **2-V₆O₆(OH₂)¹⁻** occurs *via* a rate limiting CPET from the V^{III}-OH₂ terminus.

There are limited examples of O₂ reduction *via* CPET. ORR by **2-V₆O₆(OH₂)¹⁻** is reminiscent of the mechanism previously investigated by our group for [V₆O₇(OH)₆(TRIS^{NO2})₂]²⁻.¹⁶ These POV-alkoxides are unique because they facilitate ORR from adsorbed H-atoms on the cluster surface. We therefore attribute CPET reactivity to the H⁺/e⁻ originating from the same bond (*i.e.* bridging hydroxide or terminal aquo). This observed preference for CPET ORR by both **2-V₆O₆(OH₂)¹⁻** and [V₆O₇(OH)₆(TRIS^{NO2})₂]²⁻ may be credited to the thermodynamic preference to avoid energetically costly charged intermediates, a consequence of strong thermodynamic coupling of the proton and electron. Additionally, while at first glance the rates of ORR by the two POV-alkoxides seem similar, considering the number of available H-atoms available to react with O₂ (2 for **2-V₆O₆(OH₂)¹⁻** and 6 for [V₆O₇(OH)₆(TRIS^{NO2})₂]²⁻, the aquo-bound complex in fact reacts ~4 times faster ($1.8 \times 10^{-5} \text{ M s}^{-1}$ and $5.0 \times 10^{-6} \text{ M s}^{-1}$). This acceleration could be accounted for by the driving forces for 2H⁺/2e⁻ transfer to O₂; ORR by **2-V₆O₆(OH₂)¹⁻** is 1.5 kcal mol⁻¹ more thermodynamically downhill, though we cannot rule out the effect of site-specific reactivity in accelerating the rate. The H-atoms in [V₆O₇(OH)₆(TRIS^{NO2})₂]²⁻ are located across the six equatorial bridging oxides of the Lindqvist core, meaning that an O₂ molecule would need to migrate

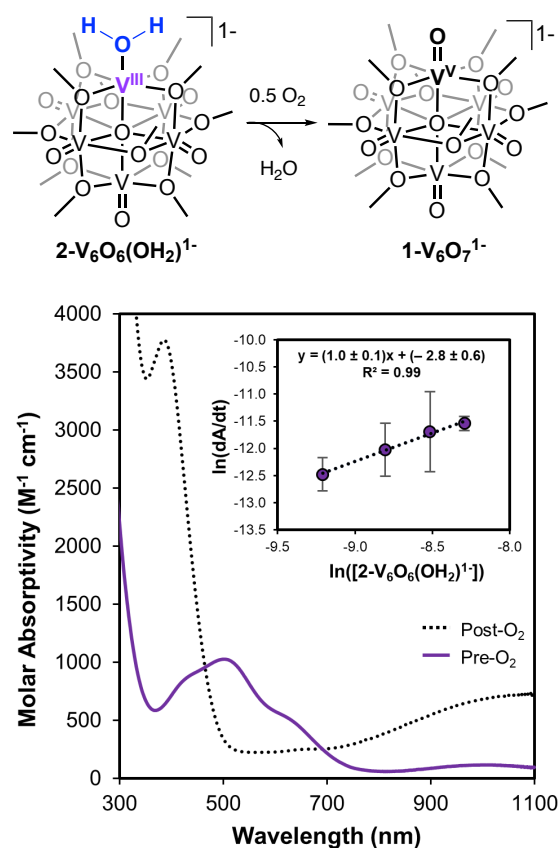


Figure 3. a. Initial and final EAS scans for the oxidation of **2-V₆O₆(OH₂)¹⁻**. Inset shows Log-log plot of the rate versus **2-V₆O₆(OH₂)¹⁻**.

between each CPET step. By localizing both reducing equivalents, ORR at $2\text{-V}_6\text{O}_6(\text{OH}_2)^{1-}$ requires little to no movement of O_2 , accelerating the reaction. Therefore, the implication for the design of MO_x is to generate bound H-atoms to terminal or bridging sites to accelerate reaction rates by pushing the mechanism towards CPET.

Here, the terminal $\text{V}^{\text{III}}\text{-OH}_2$ site on $2\text{-V}_6\text{O}_6(\text{OH}_2)^{1-}$ is found to be capable of mediating hydrogenation reactions *via* CPET for small molecule substrates (*e.g.* TEMPO, O_2). After establishing reactivity, we employ our POV-alkoxide clusters as molecular models for ORR to explore the effect of H-atoms bound at bridging vs terminal oxide sites. Ultimately, both O-H sites yield CPET mediated ORR, suggesting that adsorbed H-atoms dictate the preferred mechanism. This work presents a new synthetic strategy to improve ORR by incorporating bound H-atoms on the surface of MO_x .

This research was funded by the National Science Foundation (CHE-2154727). B.M.F. performed investigations with TEMPO, all other experiments were performed by S.E.C and E.S. All authors contributed to the writing of the manuscript. We acknowledge Dr. Kamaless Patra for kinetic discussions and Kathryn R. Proe for assistance in data collection.

Conflicts of interest

There are no conflicts to declare.

Notes and references

† Authors contributed equally.

- Y. He, S. Liu, C. Priest, Q. Shi and G. Wu, *Chemical Society Reviews*, 2020, **49**, 3484-3524.
- R. Lin, X. Cai, H. Zeng and Z. Yu, *Advanced Materials*, 2018, **30**, 1705332.
- M. Shao, Q. Chang, J.-P. Dodelet and R. Chenitz, *Chemical Reviews*, 2016, **116**, 3594-3657.
- W. T. Hong, M. Risch, K. A. Stoerzinger, A. Grimaud, J. Suntivich and Y. Shao-Horn, *Energy & Environmental Science*, 2015, **8**, 1404-1427.
- Y. Wang, J. Li and Z. Wei, *Journal of Materials Chemistry A*, 2018, **6**, 8194-8209.
- C. Goswami, K. K. Hazarika and P. Bharali, *Materials Science for Energy Technologies*, 2018, **1**, 117-128.
- S. Chakraborty, B. E. Petel, E. Schreiber and Ellen M. Matson, *Nanoscale Advances*, 2021, **3**, 1293-1318.
- D.-L. Long, E. Burkholder and L. Cronin, *Chemical Society Reviews*, 2007, **36**, 105-121.
- D.-L. Long, R. Tsunashima and L. Cronin, *Angewandte Chemie International Edition*, 2010, **49**, 1736-1758.
- Y.-F. Song and R. Tsunashima, *Chemical Society Reviews*, 2012, **41**, 7384-7402.
- M. T. Pope and A. Müller, *Angewandte Chemie International Edition in English*, 1991, **30**, 34-48.
- C. W. Anson and S. S. Stahl, *Chemical Reviews*, 2020, **120**, 3749-3786.
- M. R. Horn, A. Singh, S. Alomari, S. Goberna-Ferrón, R. Benages-Vilau, N. Chodankar, N. Motta, K. Ostrikov, J. MacLeod, P. Sonar, P. Gomez-Romero and D. Dubal, *Energy & Environmental Science*, 2021, **14**, 1652-1700.
- I. V. Kozhevnikov, Y. V. Burov and K. I. Matveev, *Bulletin of the Academy of Sciences of the USSR, Division of chemical science*, 1981, **30**, 2001-2007.
- Y. V. Geletii, C. L. Hill, R. H. Atalla and I. A. Weinstock, *Journal of the American Chemical Society*, 2006, **128**, 17033-17042.
- A. A. Fertig, W. W. Brennessel, J. R. McKone and E. M. Matson, *Journal of the American Chemical Society*, 2021, **143**, 15756-15768.
- C. Y. M. Peter, E. Schreiber, K. R. Proe and E. M. Matson, *Dalton Transactions*, 2023, **52**, 15775-15785.
- S. E. Cooney, A. A. Fertig, M. R. Buisch, W. W. Brennessel and E. M. Matson, *Chemical Science*, 2022, **13**, 12726-12737.
- B. E. Petel, W. W. Brennessel and E. M. Matson, *Journal of the American Chemical Society*, 2018, **140**, 8424-8428.
- B. E. Petel and E. M. Matson, *Chemical Communications*, 2020, **56**, 13477-13490.
- S. E. Cooney, E. Schreiber, W. W. Brennessel and E. M. Matson, *Inorganic Chemistry Frontiers*, 2023, **10**, 2754-2765.
- E. Schreiber, W. W. Brennessel and E. M. Matson, *Inorganic Chemistry*, 2022, **61**, 4789-4800.
- R. G. Agarwal, S. C. Coste, B. D. Groff, A. M. Heuer, H. Noh, G. A. Parada, C. F. Wise, E. M. Nichols, J. J. Warren and J. M. Mayer, *Chemical Reviews*, 2022, **122**, 1-49.
- P. Mondal, I. Ishigami, E. F. Gérard, C. Lim, S.-R. Yeh, S. P. de Visser and G. B. Wijeratne, *Chemical Science*, 2021, **12**, 8872-8883.
- O. Snir, Y. Wang, M. E. Tuckerman, Y. V. Geletii and I. A. Weinstock, *Journal of the American Chemical Society*, 2010, **132**, 11678-11691.
- T. H. Parsell, M.-Y. Yang and A. S. Borovik, *Journal of the American Chemical Society*, 2009, **131**, 2762-2763.
- J. Amtawong, B. B. Skjelstad, D. Balcells and T. D. Tilley, *Inorganic Chemistry*, 2020, **59**, 15553-15560.
- E. Schreiber, A. A. Fertig, W. W. Brennessel and E. M. Matson, *Journal of the American Chemical Society*, 2022, **144**, 5029-5041.
- N. Kindermann, C.-J. Günes, S. Dechert and F. Meyer, *Journal of the American Chemical Society*, 2017, **139**, 9831-9834.
- T. G. Carrell, P. F. Smith, J. Dennes and G. C. Dismukes, *Physical Chemistry Chemical Physics*, 2014, **16**, 11843-11847.
- A. Chellmani and R. Suresh, *Reaction Kinetics and Catalysis Letters*, 1988, **37**, 501-505.
- A. S. Ivanova, A. D. Merkuleva, S. V. Andreev and K. A. Sakharov, *Food Chemistry*, 2019, **283**, 431-436.
- R. L. Meyer, P. Miró, W. W. Brennessel and E. M. Matson, *Inorganic Chemistry*, 2021, **60**, 13833-13843.
- R. Tyburski, T. Liu, S. D. Glover and L. Hammarström, *Journal of the American Chemical Society*, 2021, **143**, 560-576.
- M. L. Pegis, C. F. Wise, D. J. Martin and J. M. Mayer, *Chemical Reviews*, 2018, **118**, 2340-2391.
- D. Vasudevan and H. Wendt, *Journal of Electroanalytical Chemistry*, 1995, **392**, 69-74.